ASIAN JOURNAL OF PHARMACEUTICAL AND CLINICAL RESEARCH

INNOVARE ACADEMIC SCIENCES
Knowledge to Innovation

Vol 19, Issue 2, 2026

Online - 2455-3891
Print - 0974-2441

Research Article

THIOSEMICARBAZONE − BASEDZN(II), CU(II),NI(II) AND CO(II) COMPLEXES: SYNTHESIS, CHARACTERIZATION AND EVALUATION OFANTIBACTERIAL AND ANTIFUNGALACTIVITIES

DEEPIKA SIHAG, PURNIMA NAG*

Department of Chemistry, Jaipur National University, Jaipur, Rajasthan, India.
***Corresponding Author: Purnima Nag; Email: purnima_nag007@yahoo.com**

Received: 29 October 2025, Revised and Accepted: 26 December 2025

ABSTRACT

Objective: The aim of the research is to synthesis, characterize and evaluate the biological activity of Cu(II), Zn(II), Co(II) and Ni(II) complex from thiosemicarbazone (TSC) ligands.

Methods: The ligands were synthesised by refluxing thiosemicarbazide with 2-acetylfuran in water, forming a dark brown product. The complexation reaction involved stirring aqueous solutions of Cu(II), Zn(II), Co(II) and Ni(II) salts with an ethanolic solution of Schiff base ligand. These metal complexes were tested for their anti-fungal and anti-bacterial activity against selected fungal and bacterial strains.

Results: The complexes were studied using infrared (IR), nuclear magnetic resonance and Mass spectroscopy. IR spectra showed that the nitrogen (of azomethine) and atoms of sulfur coordinated the ligands. Metal complexes activity has superior antifungal and antibacterial as compared to free ligands, perhaps due to lipophilicity and chelation. Zinc(II) complexes had the highest activity, followed by Cu(II), Ni(II) and Co(II) complexes, demonstrating the role of the central metal ion in biological characteristics.

Conclusion: The obtained outcomes specified that the produced complexes of metal with TSC may be attractive candidates for novel antibacterial and antifungal medicines, requiring additional biological investigations.

Keywords: Synthesis, Thiosemicarbazone, Metal complexes, Anti-microbial activity, Anti-fungal activity.

 DOI: http://dx.doi.org/10.22159/ajpcr.2026v19i2.57257. Journal homepage: https://innovareacademics.in/journals/index.php/ajpcr

INTRODUCTION

The study of transition metals with Schiff bases in terms of coordination chemistry has been a significant field of study in recent years, mostly due to their electrical characteristics, ease of availability, and ease of synthesis. Schiff bases in terms of coordination chemistry during modern times has secured key consideration owing to their extensive scope of applications such as optically active material [1], catalytic [2], antibacterial activity [3-5], antifungal [6], thermal studies [7], agriculture [8,9], anticancer activity [10], toxicity [11], antiviral [12] as well as DNA binding [13]. In this family of chemicals, the imine (C=N) group is crucial for biological action. The coordination molecules of thiosemicarbazone (TSC) Schiff bases in combination with transition metals have attracted interest due to their ability to inhibit DNA synthesis [14]. Moreover, the addition of ketones or aldehydes to TSC results in the formation of Schiff bases, which may interact with metal ions to create complexes exhibiting stable coordination numbers of four, five, or six [15,16]. TSC Schiff-based ligands are known for their ability to create complexes that coordinate with transition metal ions [17].

Thiosemicarbazide is a fundamental hydrazine analog of thiocarbamic acid. (NH_2-NH-$CSNH_2$) [18]. Thiosemicarbazides are commonly utilized in pharmaceutical chemistry as efficient intermediates for synthesizing pharmaceutical and bioactive compounds [19]. They are synthesized by reacting thiosemicarbazide with aldehyde or ketone [20]. TSCs binds to S-atom and N-atom of hydrazine and act as chelating ligands for transition metal ions. TSCs and related complexes have expanded important attention due to their pharmacological properties [21].

TSCs have long been recognized as a significant category of ligands for a variety of explanations, including varied donor characteristics, structural diversity, and biological uses [22]. TSC ligands and analogs containing metal complexes of them have been shown to have remarkable therapeutic qualities and emerged to be advantageous for developing more potent and less toxic medications. According to the literature, metals are selective for specific cells, and how they coordinate affects ligand binding to proteins and enzymes [23]. Several biological activities of analogs of TSC metal complexes are summarized in Fig. 1 [24].

Several transition metal complexes with biological activity have been extensively studied. Ferrocene (having Fe), a powerful organometallic molecule, has been combined with other chemicals to improve biological activity, including antimalarial and anticancer properties [25]. The advancement in the creation of organometallic titanium-based compounds, such as Titanocenes (having Ti(II)) with a focus on assessing their cytotoxic activity and effective against breast and gastrointestinal cancer [26-28].

This study specifically hypothesizes that coordinating the TSC ligand derived from 2-acetyl furan to Zn(II), Cu(II), Ni(II), and Co(II) complexes with enhanced antibacterial and antifungal activities compared to the parent ligand, due to the synergistic effect of metal chelation, which can increase lipophilicity and membrane permeability. The primary objectives are to synthesize and thoroughly characterize these complexes and to systematically evaluate their bioactivity against a panel of bacterial and fungal strains. The unique contribution of this work lies in the specific selection of the 2-acetyl furan-TSC scaffold, a ligand system which remains underexplored for first-row transition metal complexes despite of having the favorable pharmacokinetic profile imparted by the furan heterocycle. This constitutes the first comprehensive report on the biological efficacy of this particular ligand's Zn, Cu, Ni, and Co complexes, thereby filling a defined gap in the literature on furan-based metallo-antimicrobials.

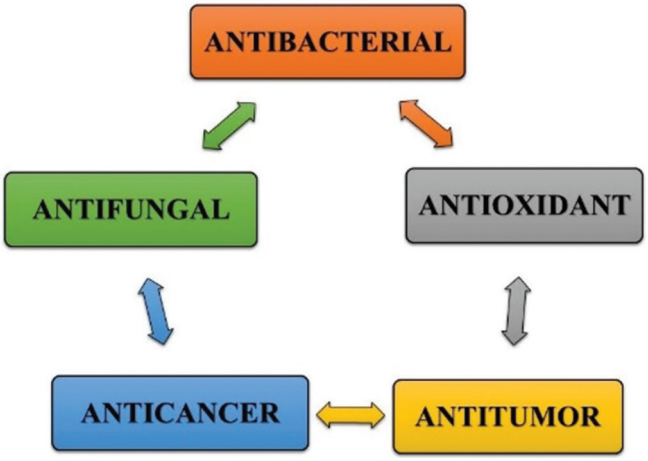

Fig. 1: Biological activities of thiosemicarbazone metal complexes analogs

METHODS

All the reagents and chemicals were procured from MERCK, and no further purification was done. Infrared (IR) spectra were documented using a Fourier transform IR spectrophotometer of Perkin-Elmer-1650 in the zone of 4000–200 cm^{-1}, and potassium bromide was used as blank. Internal reference was TMS used for recording spectra of ^{1}H-nuclear magnetic resonance (NMR) using dimethyl sulfoxide (DMSO)-D6 solvent, on DELTA2_NMR spectrophotometer. The spectral analyses of ^{13}C-NMR, ^{1}H-NMR and IR studies were examined at Accuphychem Analytics, Jaipur.

Preparation of D4 ligand(E)-2-(1-(furan-2-yl)ethylidene) hydrazinecarbothioamide

Hot aqueous solution (20 mL) of 2-acetyl furan (2.416 g, 21.941 mmol) was added to an aqueous solution (20 mL) of thiosemicarbazide (2.000 g, 21.946 mmol) in the presence of sodium hydroxide (0.364 g, 9.000 mmol). The ensuing reaction mixture was vigorously agitated for three to 4 h, yielding a colored product that was then filtered and dried.

Synthesis of metal-ligand complexes

Synthesis of D4-nickel complex (M3A)

The hot aqueous solution (20 mL) of Nickel chloride (0.648 g, 2.728 mmol) mixed with ethanolic solution of respective ligand (1.000 g, 5.457 mmol). Refluxed for 3-4 hrs and a light green complex was obtained, which was washed with 50% ethanolic solution. Then, the product obtained was filtered and dried. Similar procedure was followed for the synthesis of cobalt(M3B), copper(M3C) and zinc(M3D) complexes.

Spectrophotometric analysis of synthesized complexes

The synthesized complexes are assessed for physical and analytical data such as color, melting point, chemical analysis, and spectrophotometric techniques such as IR, 1H NMR, and high-resolution mass spectrometry to determine their structural conformation.

Method for antibacterial evaluation

The antibacterial activity of the synthesized compounds was assessed using the well diffusion technique. *Escherichia coli* and *Staphylococcus aureus* subcultures were cultivated in nutritive Agar for 24 h at 37°C. The cultures were then transferred onto petri plates that contained nutritional agar using a cotton swab that had been sterilized. Wells with a diameter of 6 mm were punched on agar plates, and samples with a concentration of 25–100 µg/mL were added. Following incubation, the zone of inhibition in each well was determined. Streptomycin (30 µg/mL) was used as a control to examine the samples' effectiveness against the bacteria under investigation. To calculate the activity index (AI), the inhibition zone (IZ) of the test sample was divided by the IZ of the antibiotic medication. Three duplicates of each experiment were carried out.

Table 1: Physical findings of ligand and their complexes

Name	Color	%Yield	Melting point (°C)
D4	Dark brown	75	160–165
M3A	Light green	61	197
M3B	Blue	60	160–170
M3C	Light brown	64	180–185
M3D	Dark brown	68	195–200

Table 2: The spectral outcomes of infrared of the synthesized ligand and their complexes (readings in cm^{-1})

Name	s (N-H)	s (C=N)	s (C=O; furan ring)	s (C=S)	v (M-N)
D4	3451	1620	1280	754	-
M3A	3257	1613	1318	1402	608
M3B	3284	1608	1282	1418	631
M3C	3404	1596	1283	1283	592
M3D	3416	1617	1417	1417	581

Table 3: 1H-nuclear magnetic resonance spectral results

Name	Chemical shifts (δ in ppm)
D4	δ 10.23 (s, 1H), 8.23 (s, 1H), 7.71 (dd, J=1.9, 0.8 Hz, 1H), 7.65 (s, 1H), 7.05 (dd, J=3.5, 0.8 Hz, 1H), 6.54 (dd, J=3.5, 1.8 Hz, 1H), 2.19 (s, 3H)
M3A	δ 10.08 (s, 1H), 8.08 (s, 1H), 7.58 (s, 2H), 6.92 (s, 2H), 6.41 (s, 2H), 2.05 (s, 5H)
M3B	δ 10.12 (s, 1H), 8.08 (s, 1H), 7.79 (s, 1H), 7.67 (s, 2H), 7.01 (d, J=3.4 Hz, 2H), 6.51 (dd, J=3.4, 1.7 Hz, 2H), 2.19 (s, 5H)
M3D	δ 10.23 (s, 1H), 8.23 (s, 1H), 7.71 (dd, J=1.8, 0.8 Hz, 1H), 7.65 (s, 1H), 7.06 (dd, J=3.5, 0.9 Hz, 1H), 6.55 (dd, J=3.4, 1.8 Hz, 1H), 2.19 (s, 2H)

Table 4: ^{13}C-Nuclear magnetic resonance spectral results

Name	Chemical shifts (δ in ppm)
D4	δ 178.99, 178.40, 152.09, 148.89, 145.88, 144.63, 140.46, 134.16, 116.21, 112.49, 112.31, 110.99, 40.43, 40.22, 40.01, 39.80, 39.59, 39.38, 39.17, 20.81, 13.65.
M3A	δ 155.78, 148.96, 144.57, 116.47, 115.19, 18.09.
M3B	δ 156.51, 151.17, 150.05, 146.00, 117.42, 116.31, 19.10.
M3D	δ 178.84, 152.09, 144.69, 140.63, 112.54, 111.08, 40.45, 40.24, 40.03, 39.82, 39.61, 39.40, 39.19, 18.92, 13.70.

Method for antifungal evaluation

At doses range of 25–100 µg/mL, the ligand metal complex's antifungal activity against two strains of *Penicillium chrysogenum* and *Fusarium oxysporum* was assessed. The plates dried at room temperature for 15 min. For 6 mm agar wells, cork-borers were utilized. A well was also made with the same distance control. The test solution of the synthesized ligand and its metal complexes was prepared in DMSO at concentrations of 25, 50, 75, and 100 µg/mL for initial antifungal screening. Various amounts of standard medicine and other substances were sowed into petri plate wells. At 28°C, seeded plates incubated for 48 h. The IZ diameter was measured in millimeters to test antifungal activity. Each experiment was repeated 3 times, and the mean value was calculated. Antifungal activity was measured using ketoconazole (30 µg/mL) as the standard control. AI was computed in addition to IZ.

RESULT AND DISCUSSION

The chemical reaction of metal chlorides with TSC in a 1:2 molar ratio results in metal-ligand complex. The suggested geometry of

synthesized metal-ligand complexes is octahedral. These synthesized compounds are soluble in DMSO solvents and have been studied through spectroscopic research. Analytical and physical findings are summarized in Table 1.

Spectrophotometric analysis of synthesized complexes

IR spectra

The IR spectra of the M3A-M3D complexes exhibit distinct and consistent modifications relative to the free ligand D4, confirming coordination through the TSC fragment and, to a lesser extent, the furan ring. The azomethine ν(C=N) and thioamide ν(C=S) bands of D4 move to lower wavenumbers in all complexes, showing the imine nitrogen and thioenolate sulfur atoms in metal binding. New absorptions in the 520–560 cm^{-1} area were ascribed to ν(M-S) vibrations, indicating direct metal-sulfur coordination. Additional weaker bands between 430 and 480 cm^{-1} belong to ν(M-N) and possibly ν(M-O) modes, similar with reported values for furan-based TSC complexes. The conservation of broad N-H absorptions lends credence to the notion

Table 5: Results of antibacterial action against *Escherichia coli* and *Staphylococcus aureus* in terms of inhibition zone

Name	*E coli* (in terms of inhibition zone)					*S. aureus* (in terms of inhibition zone)						
	Concentration (µg/mL)					Concentration (µg/mL)						
	25	50	75	100	Mean	25	50	75	100	Mean	Total Mean	SD
D4	10	13	16	18	14.3	9	11	12	14	11.5	12.9	2.8
M3A	7	8	9	10	8.5	9	10	11	13	10.8	9.6	1.5
M3B	7	8	10	11	9.0	7	8	10	11	9.0	9.0	1.8
M3C	9	14	17	20	15.0	12	13	15	17	14.3	14.6	3.5
M3D	14	18	19	21	18.0	16	17	19	21	18.3	18.1	2.6
Standard drug	24	30	31	32	29.3	31	35	36	38	35.0	32.1	3.3
Mean	11.8	15.2	17.0	18.7	15.7	14.0	15.7	17.2	19.0	16.5	16.1	

SD: Standard deviation

Table 6: Results of antibacterial action against *Escherichia coli and Staphylococcus aureus* in terms of activity index

Name	*E coli* (in terms of activity index)					*S. aureus* (in terms of activity index)						
	Concentration (µg/mL)					Concentration (µg/mL)						
	25	50	75	100	Mean	25	50	75	100	Mean	Total mean	SD
D4	0.42	0.43	0.52	0.56	0.48	0.29	0.31	0.33	0.37	0.33	0.40	0.05
M3A	0.29	0.27	0.29	0.31	0.29	0.29	0.29	0.31	0.34	0.31	0.30	0.02
M3B	0.29	0.27	0.32	0.34	0.31	0.23	0.23	0.28	0.29	0.26	0.28	0.03
M3C	0.38	0.47	0.55	0.63	0.51	0.39	0.37	0.42	0.45	0.41	0.46	0.07
M3D	0.58	0.60	0.61	0.66	0.61	0.52	0.49	0.53	0.55	0.52	0.57	0.03
Mean	0.39	0.41	0.46	0.50	0.44	0.34	0.34	0.37	0.40	0.36	0.40	

SD: Standard deviation

Table 7: Results of antifungal action against *Penicillium chrysogenum* and *Fusarium oxysporum* in terms of inhibition zone

Name	*P. chrysogenum* (in terms of inhibition zone)					*F. oxysporum* (in terms of inhibition zone)						
	Concentration (µg/mL)					Concentration (µg/mL)						
	25	50	75	100	Mean	25	50	75	100	Mean	Total Mean	SD
D4	7	9	11	13	10.0	7	8	12	14	10.3	10.1	2.94
M3A	7	8	9	10	8.5	7	8	10	12	9.3	8.9	1.75
M3B	8	10	12	14	11.0	9	12	14	16	12.8	11.9	2.78
M3C	16	18	20	23	19.3	NA	7	8	9	8.0	13.6	1.99
M3D	10	12	16	19	14.3	12	14	18	21	16.3	15.3	4.03
Standard drug	20	21	23	24	22.0	15	19	21	25	20.0	21.0	2.99
Mean	11.3	13.0	15.2	17.2	14.2	10.0	11.3	13.8	16.2	12.8	13.5	

SD: Standard deviation

Table 8: Results of antifungal action against *Penicillium chrysogenum and Fusarium oxysporum* in terms of activity index

Name	*P. chrysogenum* (in terms of activity index)					*F. oxysporum* (in terms of activity index)						
	Concentration (µg/mL)					Concentration (µg/mL)						
	25	50	75	100	Mean	25	50	75	100	Mean	Total mean	SD
D4	0.35	0.43	0.48	0.54	0.5	0.47	0.42	0.57	0.56	0.5	0.5	0.08
M3A	0.35	0.38	0.39	0.42	0.4	0.47	0.42	0.48	0.48	0.5	0.4	0.03
M3B	0.4	0.48	0.52	0.58	0.5	0.60	0.63	0.67	0.64	0.6	0.6	0.05
M3C	0.8	0.86	0.87	0.96	0.9	NA	0.37	0.38	0.36	0.4	0.6	0.04
M3D	0.5	0.57	0.7	0.79	0.6	0.80	0.74	0.86	0.84	0.8	0.7	0.09
Mean	0.48	0.54	0.59	0.66	0.57	0.59	0.52	0.59	0.58	0.57	0.6	

SD: Standard deviation

that D4 mostly functions as a neutral N, S donor, with furan oxygen playing a small role.

The N-H, C=N, and C-O (furan ring) stretching bands for ligands and metal complexes are detected within the anticipated ranges of 3200–3500 cm^{-1}, 1550–1650 cm^{-1}, and 1200–1450 cm^{-1}, respectively. The complexes M3A-M3D show ν(N-H) bands at 3257, 3284, 3404, and 3416 cm^{-1} and ν(C=N) bands at 1613, 1608, 1596, and 1617 cm^{-1}, indicating the downward shift associated with azomethine coordination. M3A, M3B, M3C, and M3D exhibit ν(M-N) bands at 608, 631, 592, and 581 cm^{-1}, confirming metal-nitrogen bonding (Table 2).

Proton NMR and ^{13}C-NMR spectra

The ligand (D4) and metal complex (M3A, M3Band M3D) were analyzed for proton NMR and ^{13}C NMR was shown in Tables 3 and 4, respectively. In proton NMR, hydrogen for primary amine was found to be 6.92, 7.01, and 6.55 for M3A, M3B, and M3D, respectively. A singlet for methyl was observed at 2.05, 2.19, and 2.19 forM3A, M3B, and M3D, respectively. A peak for -NH was found at 10.08, 10.12, and 10.23 for M3A, M3B, and M3D, respectively. After the formation of complex C=S will convert to C-S. For ^{13}C NMR, a peak for C-S was observed at 155.78, 156.51, and 152.09 for M3A, M3B, and M3D, respectively. For C-O, it was seen at 144.57, 151.17, and 144.69 for M3A, M3B, and M3D, respectively.

The structure of M3C is now supported exclusively by IR spectroscopy, which is appropriate for paramagnetic systems. The ligand's characteristic N–H, C=N, and C–O stretches (3200–3500, 1550–1650, and 1200–1450 cm^{-1}) shift systematically upon coordination. In M3C, the N–H band appears at 3404 cm^{-1}, the azomethine C=N shifts to 1596 cm^{-1}, and diagnostic changes occur in the C–O region. A new band at 592 cm^{-1} confirms Cu–N bond formation. These spectral features collectively validate the proposed N, S-donor coordination and confirm the structure of the Cu(II) complex.

Mass spectroscopy

The mass spectrum of D4 ligand (Fig. S14) displays a prominent molecular ion peak at m/z 184.0573, corresponding to the (M+H) species. This value agrees with the expected molecular mass of D4 ligand and confirms its molecular composition.

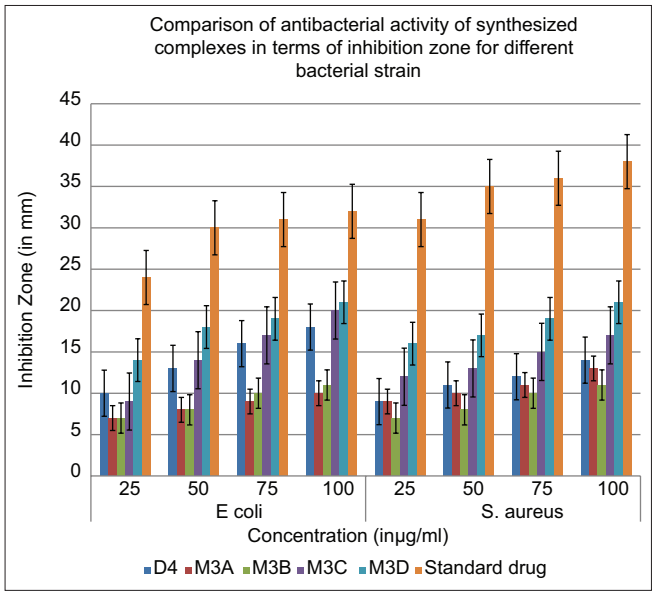

Fig. 2: Comparison graph for antibacterial activity for *Escherichia coli* and *Staphylococcus aureus* as per measured inhibition zone

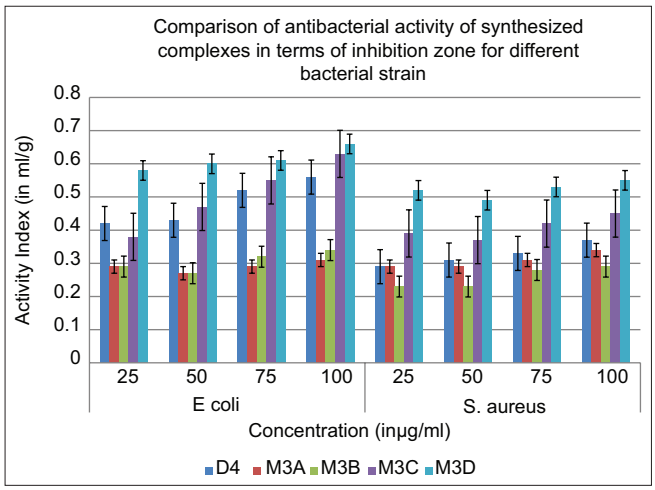

Fig. 3: Comparison graph for antibacterial activity for *Escherichia coli and Staphylococcus aureus* as per measured activity index

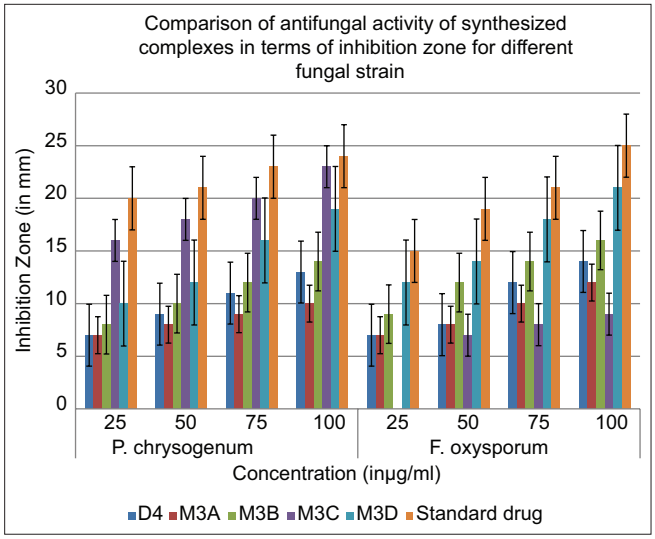

Fig. 4: Comparison graph for antifungal activity for *Penicillium chrysogenum* and *Fusarium oxysporum* as premeasured inhibition zone

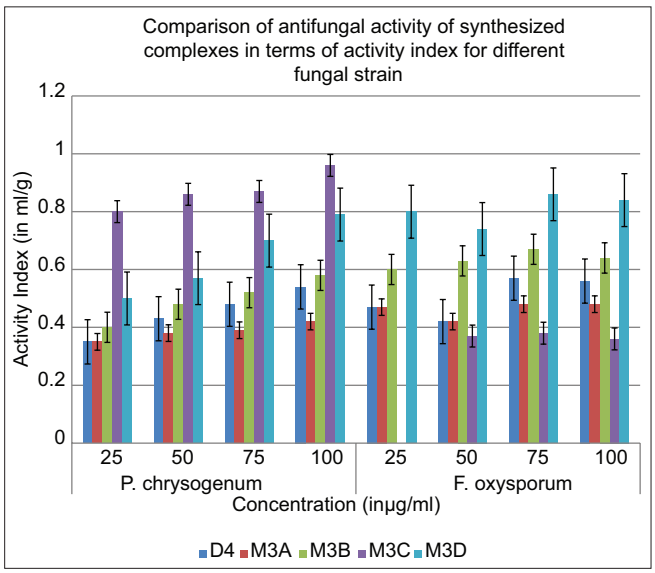

Fig. 5: Comparison graph for antifungal activity for *Penicillium chrysogenum* and *Fusarium oxysporum* as peractivity index

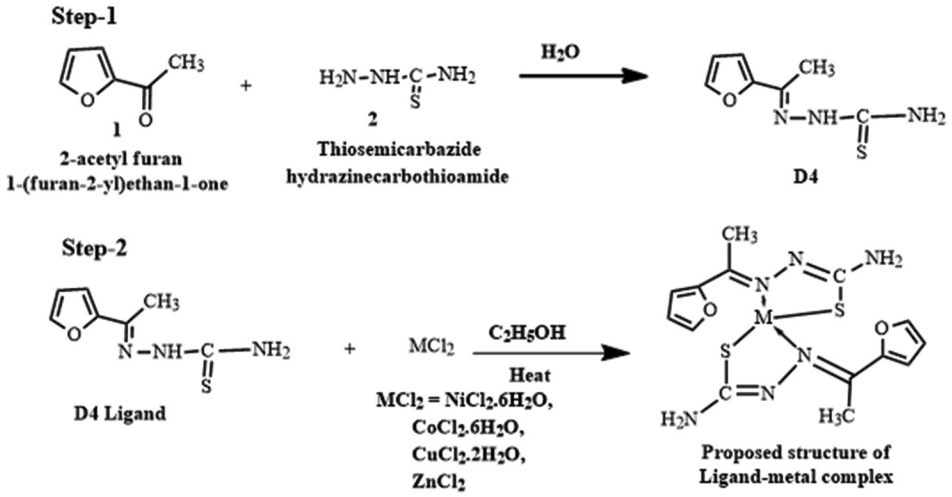

Scheme 1: Green synthesis of ligand and metal-ligand complexes

Antibacterial and antifungal activity

The ligand metal complex was analyzed for anti-bacterial activity for two strains, that is, *E. coli* and *S. aureus* at concentrations 25,50,75 and 100 µg/mL (Tables 5 and 6). The ligand and metal complex showed appreciable activity against strains (Figs. 2 and 3). The M3D complex (Zinc with ligand) shown highest activity in *E. coli* and *S. aureus* strains, Fig. S15 and S16 for antibacterial activity updated in the supplementary file.

The ligand-metal complexes underwent testing against *P. chrysogenum* and *F. oxysporum* at concentrations of 25, 50, 75, and 100 µg/mL (Tables 7 and 8). Among the complexes, M3C (Cu-ligand) demonstrated the most significant inhibition against *P. chrysogenum*, whereas M3D (Zn-ligand) displayed enhanced activity against *F. oxysporum*. The ligand and metal combination demonstrated significant action against the strains (Figs. 4 and 5). Fig.S17 and S18 in the supplementary material for the antifungal activity cultured strain.

The variation can be attributed to the unique chemical behavior exhibited by the metal ions. Cu(II) exhibits redox activity and has the potential to induce oxidative stress within fungal cells, which contributes to the enhanced inhibition noted for M3C. Zn(II) is a potent Lewis acid that can disrupt fungal enzyme systems, thereby enhancing the effectiveness of M3D against *F. oxysporum*. Furthermore, the increased lipophilicity following complexation probably improves membrane permeability for both M3C and M3D. Metal coordination typically decreases the polarity of the ligand and enhances its capacity to traverse the lipid-rich fungal cell membrane. This enhanced transport can boost the inherent biological effects of the respective metal ions, thereby reinforcing their antifungal activity.

CONCLUSION

The early *in vitro* antifungal and antibacterial evaluations of all these complexes show substantial effectiveness against all strains. The ligands have lower activity than their metal complexes. At comparable concentrations, Zinc (II) is a potent Lewis acid that can disrupt fungal enzyme system thereby enhancing the effectiveness of M3D complex outperformed other complexes of metal against *S. aureus*, *F. oxysporum, and E. coli*. For the antifungal strain, *P. chrysogenum*, M3C outperformed other metal complexes at the same dosage.

AUTHORS' CONTRIBUTIONS

Conducted experiments, Deepika Sihag; Data analysis and evaluation, Deepika Sihag and Purnima Nag; Correction and editing, Purnima Nag; wrote the paper, Deepika Sihag. All authors have read and agreed to the published version of the manuscript.

CONFLICTS OF INTEREST

The authors declare no conflicts of interest.

FUNDING

This research received no external funding.

REFERENCES

1. Abozeed A, Sayed M, Younis O, Tolba MS, Hassanien R, Kamal El-Dean AM, *et al*. Characterization and optical behavior of a new indole Schiff base using experimental data and TD-DFT/DMOl3 computations. Opt Mater. 2022;131:112594. doi: 10.1016/j.optmat.2022.112594
2. Musie G, Wei M, Subramaniam B, Busch DH. Catalytic oxidations in carbon dioxide-based reaction media, including novel CO_2-expanded phases. Coord Chem Rev. 2001;219-221:789-820. doi: 10.1016/s0010-8545(01)00367-8
3. Ali HM, El-Ossaily YA, Metwally SA, Althobaiti IO, Altaleb HA, Naffea YA, *et al*. Catalytic and multicomponent reactions for green synthesis of some pyrazolone compounds and evaluation as antimicrobial agents. ACS Omega. 2022;7(33):29142-52. doi: 10.1021/acsomega.2c03070, PMID 36033712
4. Tolba MS, Sayed M, El-Dean AM, Hassanien R, Abdel-Raheem SA, Ahmed M. Design, synthesis and antimicrobial screening of some new thienopyrimidines. Org Commun. 2021;14(4):334-45.
5. Hamed MM, Sayed M, Abdel-Mohsen SA, Saddik AA, Ibrahim OA, El-Dean AM, *et al*. Synthesis, biological evaluation, and molecular docking studies of novel diclofenac derivatives as antibacterial agents. J Mol Struct. 2023;1273:134371.
6. Mohamed GG, Omar M, Hindy AM. Metal complexes of Schiff bases: Preparation, characterization, and biological activity. Turk J Chem. 2006;30:361-82.
7. Shekaari H, Kazempour A, Khoshalhan M. Schiff base ligands and their transition metal complexes in the mixtures of ionic liquid + organic solvent: A thermodynamic study. Phys Chem Chem Phys. 2015;17(3):2179-91. doi: 10.1039/c4cp04432k, PMID 25482659
8. Fouad MR, Shamsan AQ, Abdel-Raheem SA. Toxicity of atrazine and metribuzin herbicides on earthworms (*Aporrectodea caliginosa*) by filter paper contact and soil mixing techniques. Curr Chem Lett. 2023;12(1):185-92. doi: 10.5267/j.ccl.2022.8.006
9. Pandey RK, Aggarwal S, Nath G, Kumar A, Vaferi B. Metaheuristic algorithm integrated neural networks for well-test analyses of petroleum reservoirs. Sci Rep. 2022;12(1):1-16.
10. Diedrich B, Rigbolt KT, Röring M, Herr R, Kaeser-Pebernard S, Gretzmeier C, *et al*. Discrete cytosolic macromolecular BRAF complexes exhibit distinct activities and composition. EMBO J. 2017;36(5):646-63. doi: 10.15252/embj.201694732, PMID 28093501
11. Mangamamba T, Ganorkar MC, Swarnabala G. Characterization of complexes synthesized using Schiff base ligands and their screening

for toxicity two fungal and one bacterial species on rice pathogens. Int J Inorg Chem. 2014;2014:1-22. doi: 10.1155/2014/736538
12. Pandey SN, Sriram D, Nath G, De Clercq E. Synthesis, antibacterial, antifungal and anti-HIV activity of Schiff and mannich bases of isatin with N-[6-chlorobenzothiazol-2-yl] thiosemicarbazide. Indian J Pharm Sci. 1999;61:358-61.
13. Abdel-Rahman LH, El-Khatib RM, Nassr LA, Abu-Dief AM, Ismael M, Seleem AA. Metal based pharmacologically active agents: Synthesis, structural characterization, molecular modeling, CT-DNA binding studies and *in vitro* antimicrobial screening of iron(II) bromosalicylidene amino acid chelates. Spectrochim Acta A Mol Biomol Spectrosc. 2014;117:366-78. doi: 10.1016/j.saa.2013.07.056, PMID 24001978
14. Haribabu J, Jeyalakshmi K, Arun Y, Bhuvanesh NS, Perumal PT, Karvembu R. Synthesis of Ni(II) complexes bearing indole-based thiosemicarbazone ligands for interaction with biomolecules and some biological applications. J Biol Inorg Chem. 2017;22(4):461-80. doi: 10.1007/s00775-016-1424-1, PMID 27995332
15. Muthu Tamizh MM, Cooper BF, Macdonald CL, Karvembu R. Palladium(II) complexes with salicylideneimine based tridentate ligand and triphenylphosphine: Synthesis, structure and catalytic activity in Suzuki-Miyaura cross coupling reactions. Inorg Chim Acta. 2013;394:391-400. doi: 10.1016/j.ica.2012.08.024
16. Kalita M, Bhattacharjee T, Gogoi P, Barman P, Kalita RD, Sarma B, *et al*. Synthesis, characterization, crystal structure and bioactivities of a new potential tridentate (ONS) Schiff base ligand N-[2-(benzylthio) phenyl] salicylaldimine and its Ni(II), Cu(II) and Co(II) complexes. Polyhedron. 2013;60:47-53. doi: 10.1016/j.poly.2013.04.062
17. Sharma D, Nag P. Anticandidal activity of some Zn(II) and Pb(II) complexes. Mor J Chem. 2020;8:326-31.
18. Acharya PT, Bhavsar ZA, Jethava DJ, Patel DB, Patel HD. A review on development of bio-active thiosemicarbazide derivatives: Recent advances. J Mol Struct. 2021;1226:129268. doi: 10.1016/j.molstruc.2020.129268
19. Sardari S, Feizi S, Rezayan AH, Azerang P, Shahcheragh SM, Ghavami G, *et al*. Synthesis and biological evaluation of thiosemicarbazide derivatives endowed with high activity toward *Mycobacterium bovis*. Iran J Pharm Res. 2017;16(3):1128-40. PMID 29201099
20. Jindaniya V, Mishra R, Mazumder A, Tyagi S. Synthesis and diverse pharmacological actions of thiosemicarbazide analogs: A review. Lett Drug Des Disco. 2024;21(12):2302-34. doi: 10.2174/1570180820666230614121851
21. Chandra S, Kumar A. Spectral studies on Co(II), Ni(II) and Cu(II) complexes with thiosemicarbazone (L1) and semicarbazone (L2) derived from 2-acetyl furan. Spectrochim Acta A Mol Biomol Spectrosc. 2007;66(4-5):1347-51. doi: 10.1016/j.saa.2006.04.047, PMID 16919999
22. Lobana TS, Sharma R, Bawa G, Khanna S. Bonding and structure trends of thiosemicarbazone derivatives of metals-an overview. Coord Chem Rev. 2009;253(7-8):977-1055. doi: 10.1016/j.ccr.2008.07.004
23. Gupta S, Singh N, Khan T, Joshi S. Thiosemicarbazone derivatives of transition metals as multi-target drugs: A review. Result Chem. 2022;4:100459. doi: 10.1016/j.rechem.2022.100459
24. Siddiqui EJ, Azad I, Khan AR, Khan T. Thiosemicarbazone complexes as versatile medicinal chemistry agents: A review. J Drug Deliv Ther. 2019;9(3):689-703. doi: 10.22270/jddt.v9i3.2888
25. Peter S, Aderibigbe BA. Ferrocene-based compounds with antimalaria/anticancer activity. Molecules. 2019;24(19):3604. doi: 10.3390/molecules24193604, PMID 31591298
26. Skoupilova H, Hrstka R, Bartosik M. Titanocenes as anticancer agents: Recent insights. Med Chem. 2016;13(4):334-44. doi: 10.2174/1573406412666161228113650, PMID 28031018
27. Shinde VB, Raskar MA. Synthesis and biological evaluation of benzimidazole derivatives as antimicrobial agents. Int J Curr Pharm Sci. 2019;11(6):115-8. doi: 10.22159/ijcpr.2019v11i6.36356
28. Hossain S, Islam A, Tasnim F, Hossen F, E-Zahan K, Asraf A. Antimicrobial, antioxidant and cytotoxicity study of Cu(II), Zn(II), Ni(II), and Zr(IV) complexes containing O, N Donor Schiff base ligand. Int J Chem Res. 2024;8(4):1-11. doi: 10.22159/ijcr.2024v8i4.231

SUPPLEMENTARY DATA

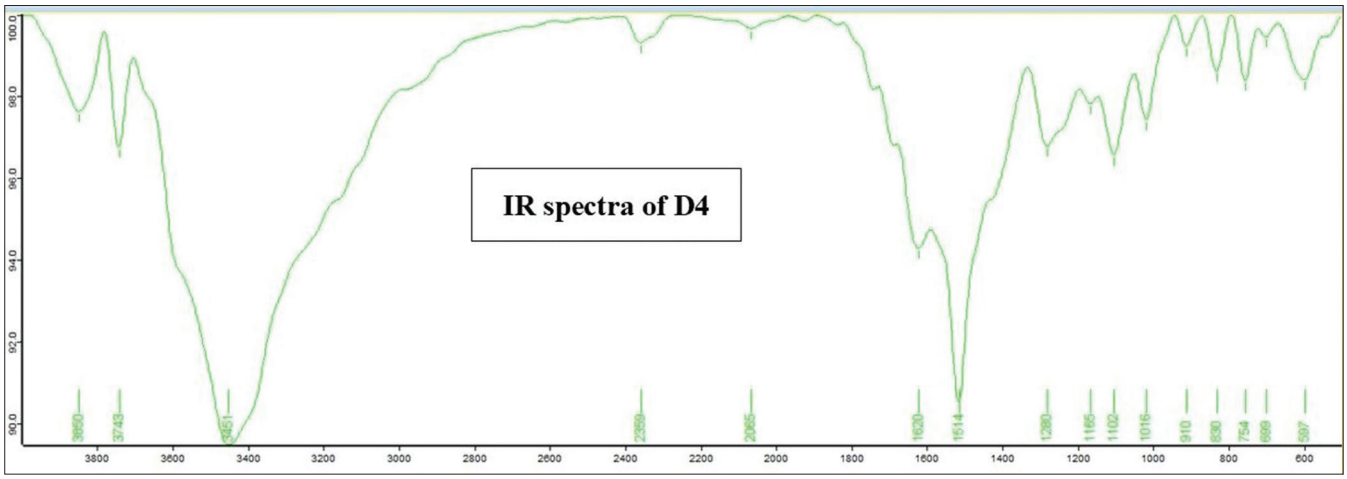

Supplementary Fig. 1: IR spectra of D4

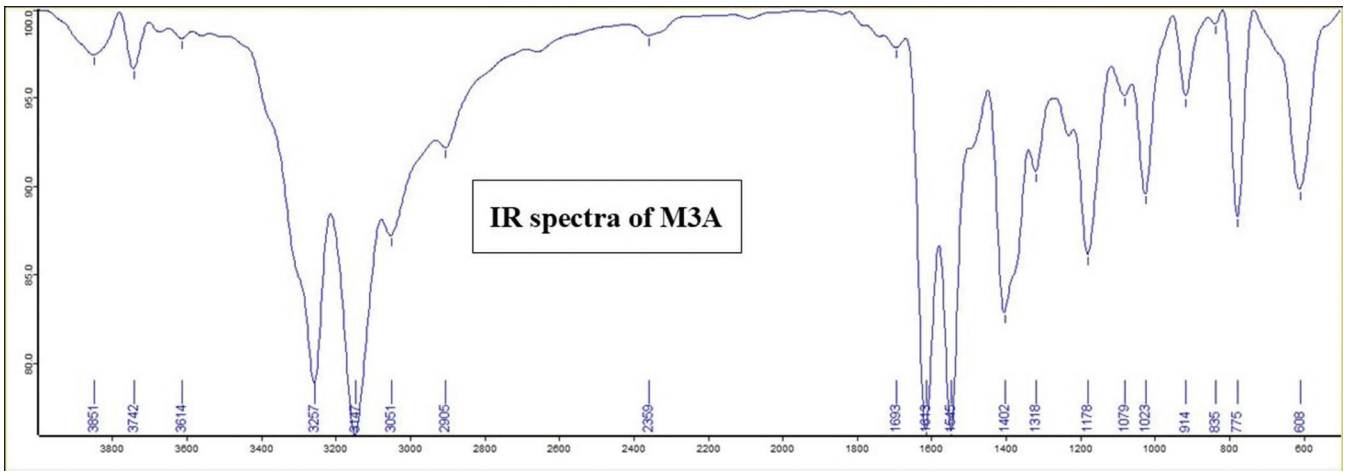

Supplementary Fig. 2: IR spectra of M3A

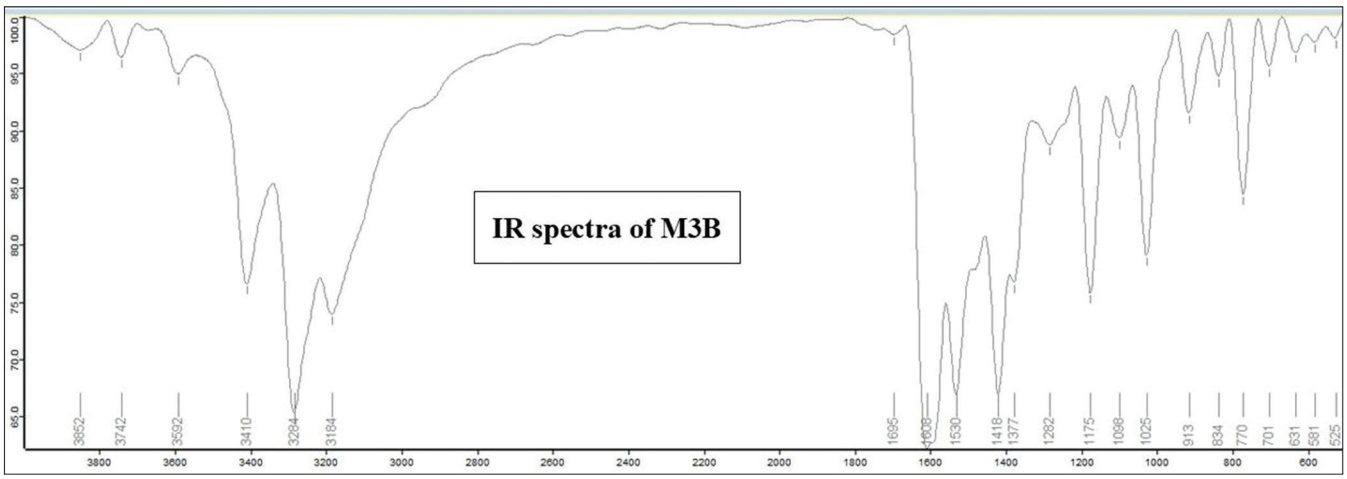

Supplementary Fig. 3: IR spectra of M3B

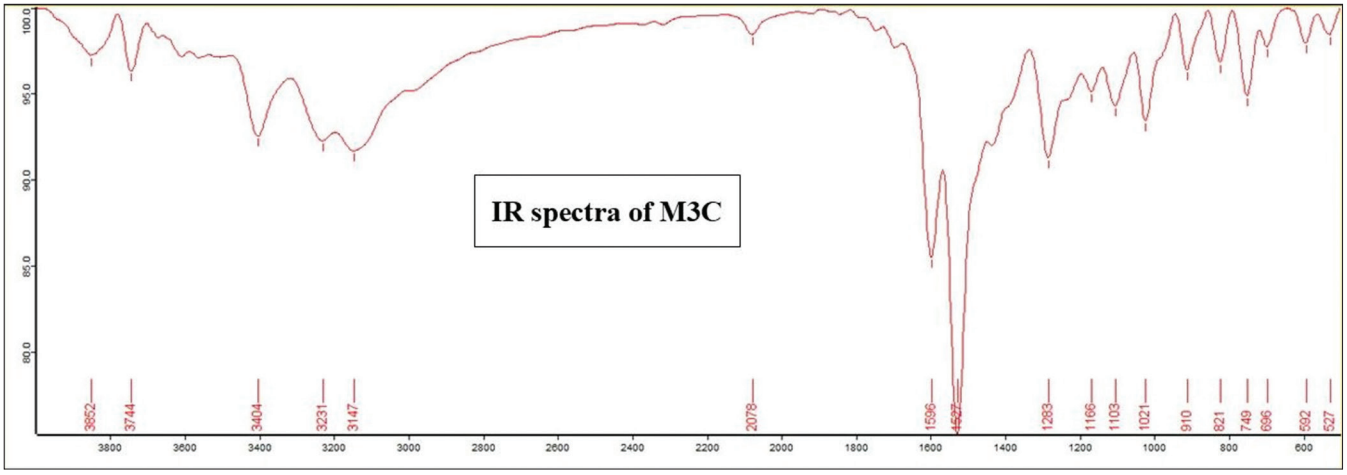

Supplementary Fig. 4: IR spectra of M3C

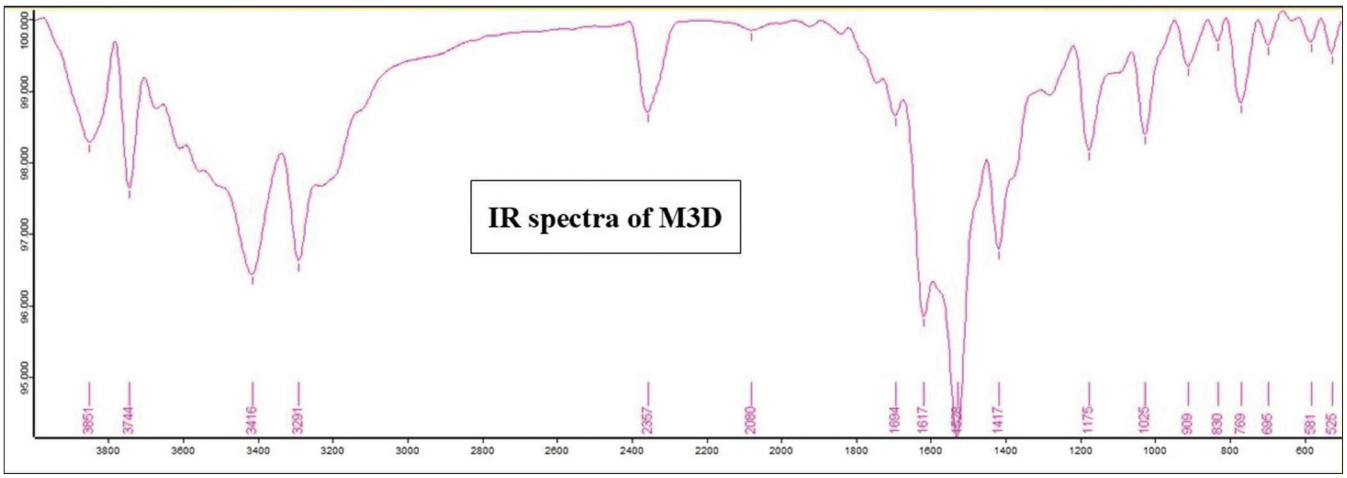

Supplementary Fig. 5: IR spectra of M3D

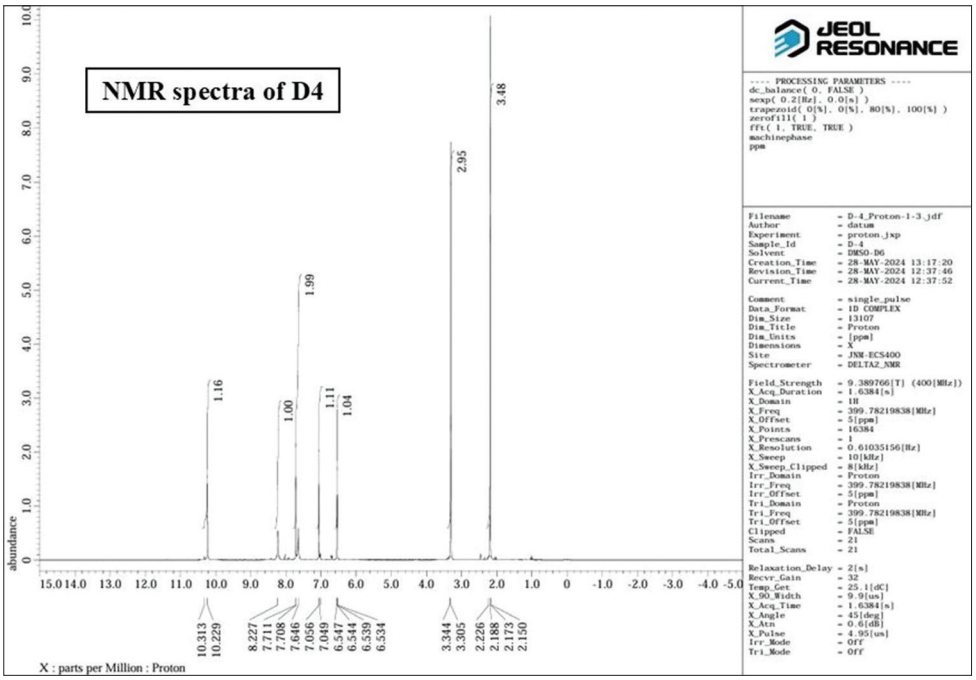

Supplementary Fig. 6: ^{1}H NMR spectra of D4

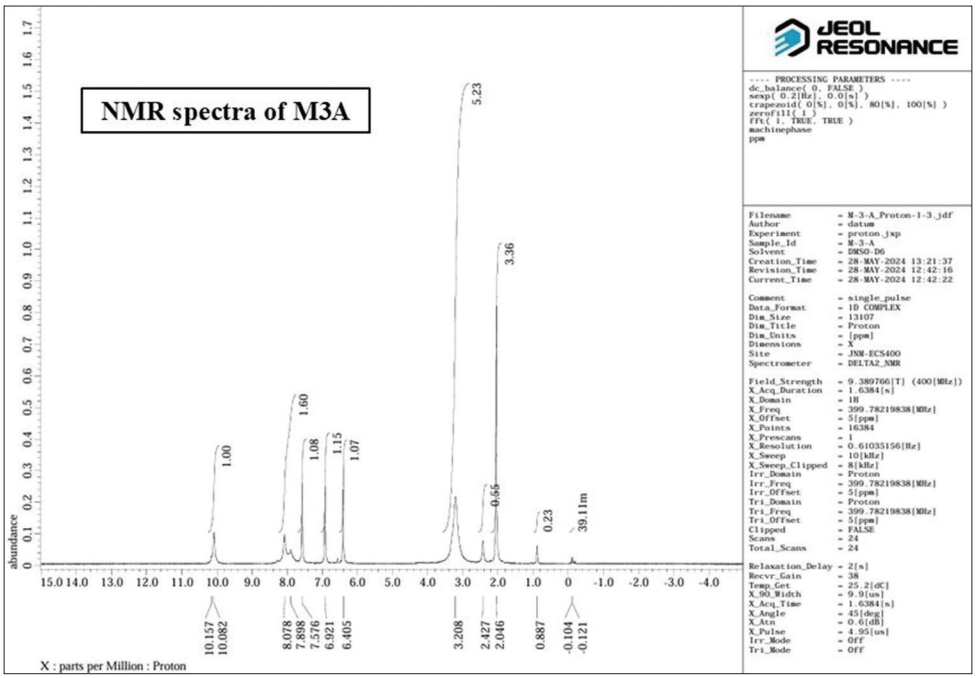

Supplementary Fig. 7: ^{1}H NMR spectra of M3A

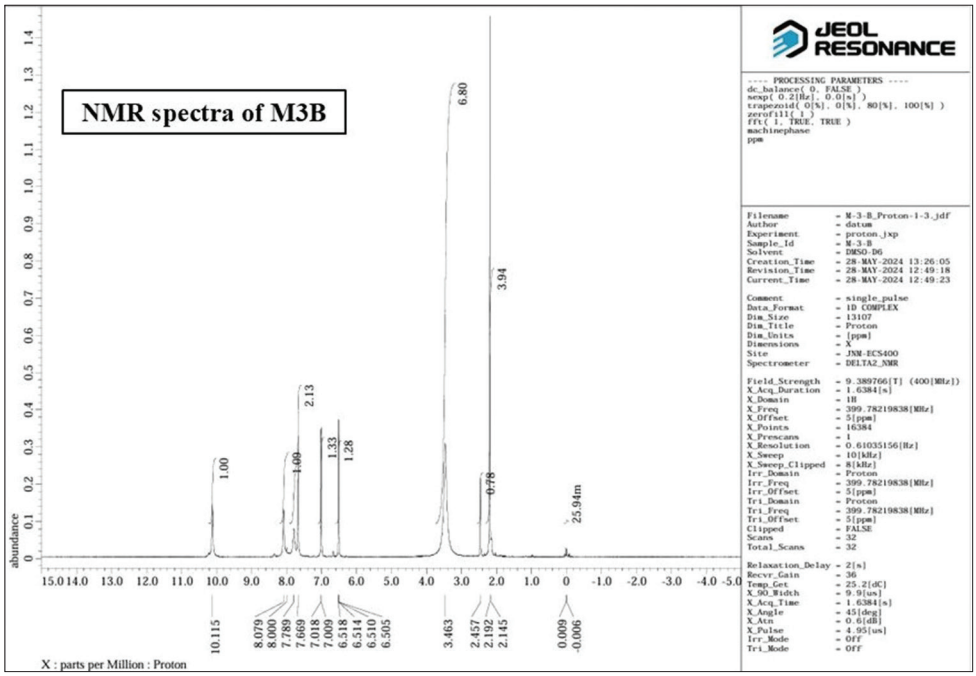

Supplementary Fig. 8: ^{1}H NMR spectra of M3B

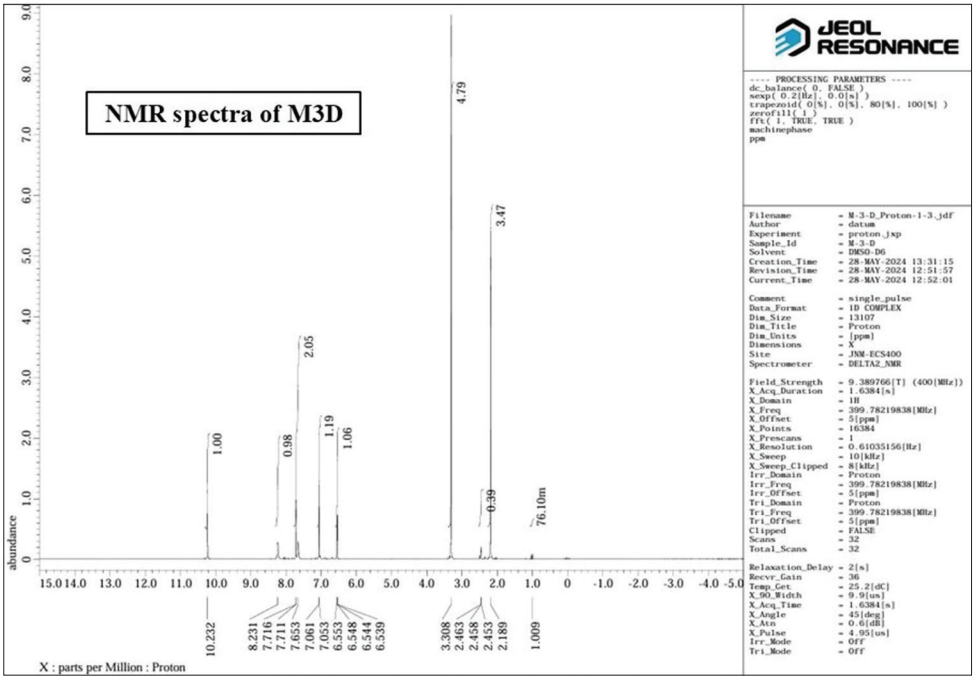

Supplementary Fig. 9: ^{1}H NMR spectra of M3D

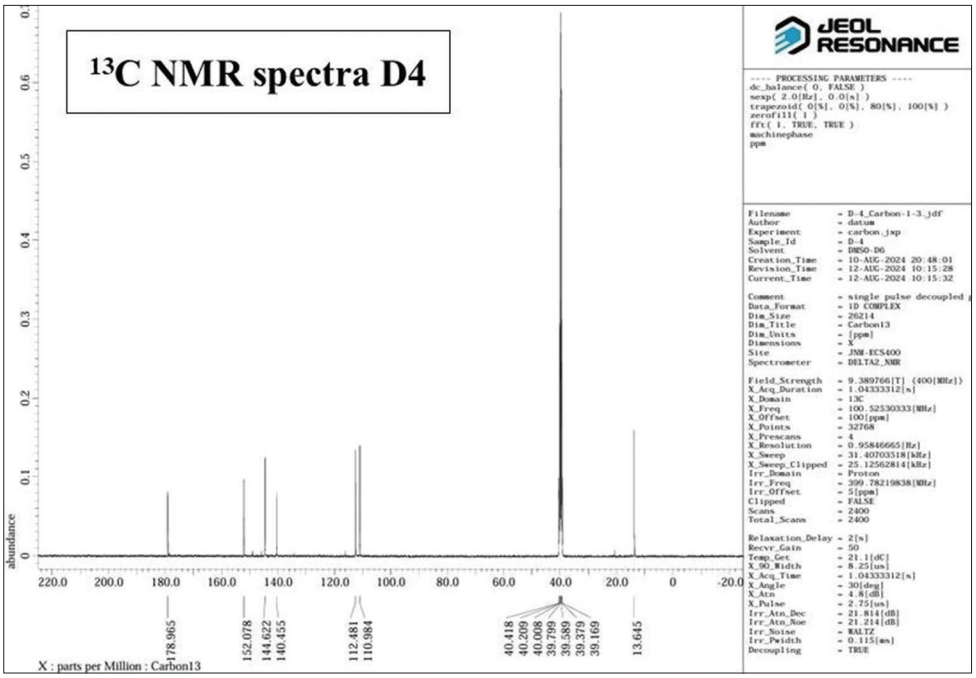

Supplementary Fig. 10: ^{13}C NMR spectra of D4

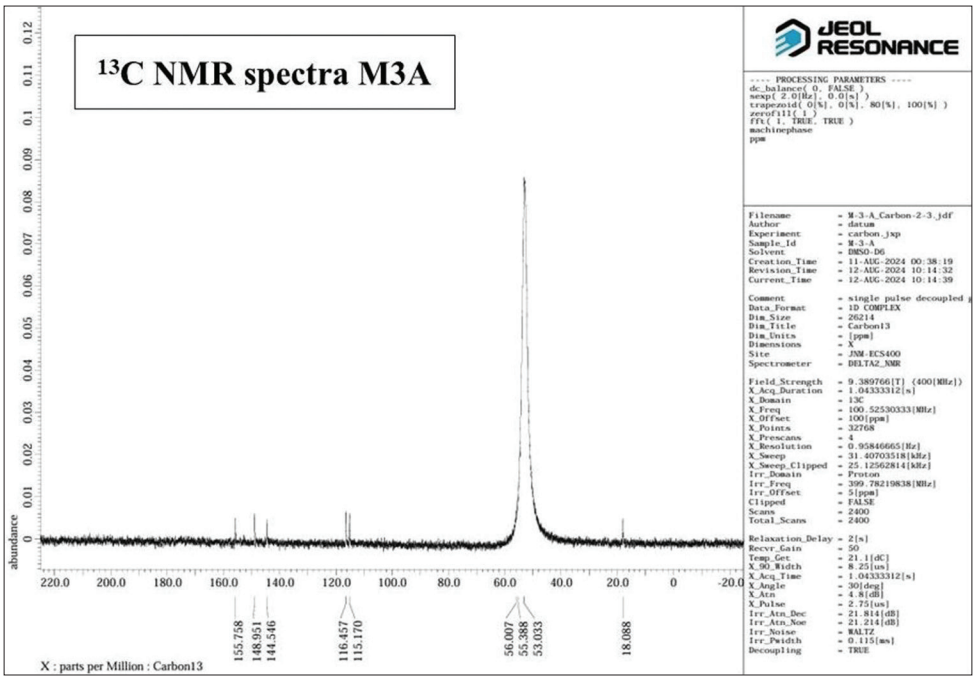

Supplementary Fig. 11: ^{13}C NMR spectra of M3A

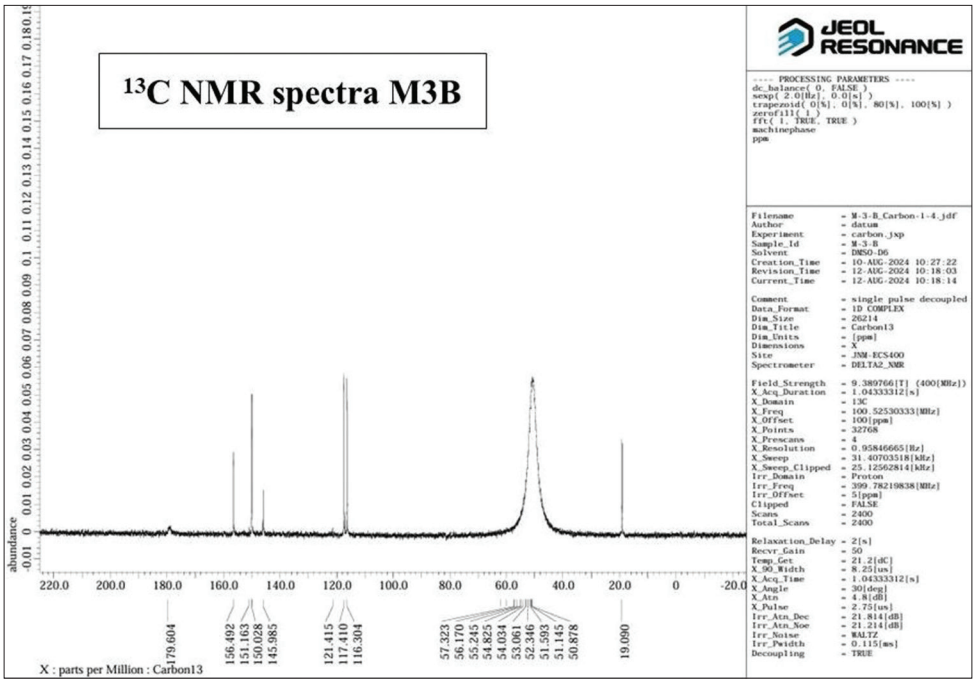

Supplementary Fig. 12: ^{13}C NMR spectra of M3B

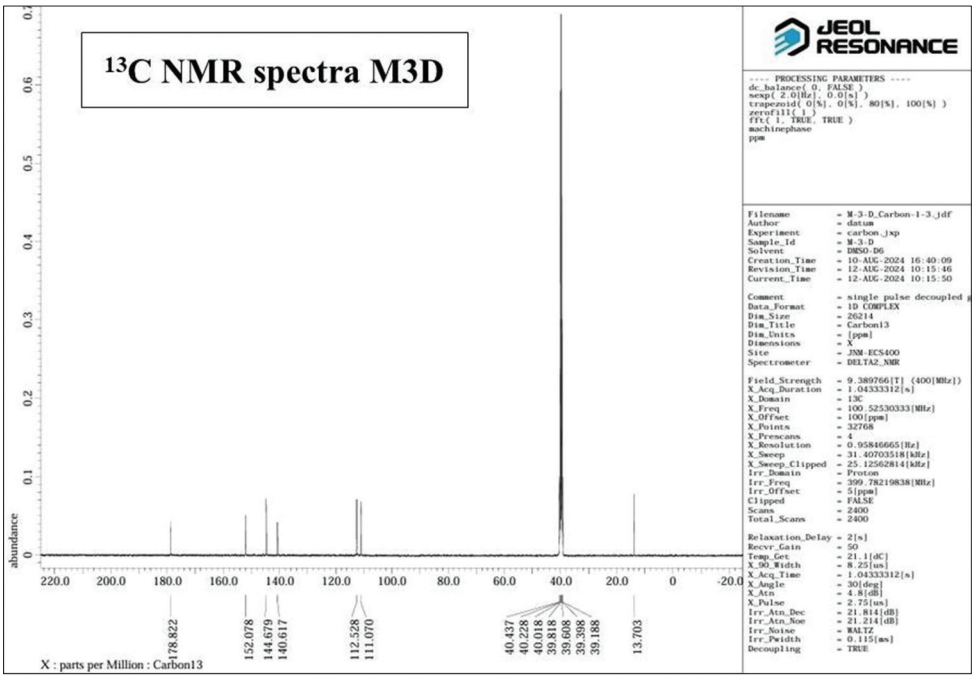

Supplementary Fig. 13: ^{13}C NMR spectra of M3D

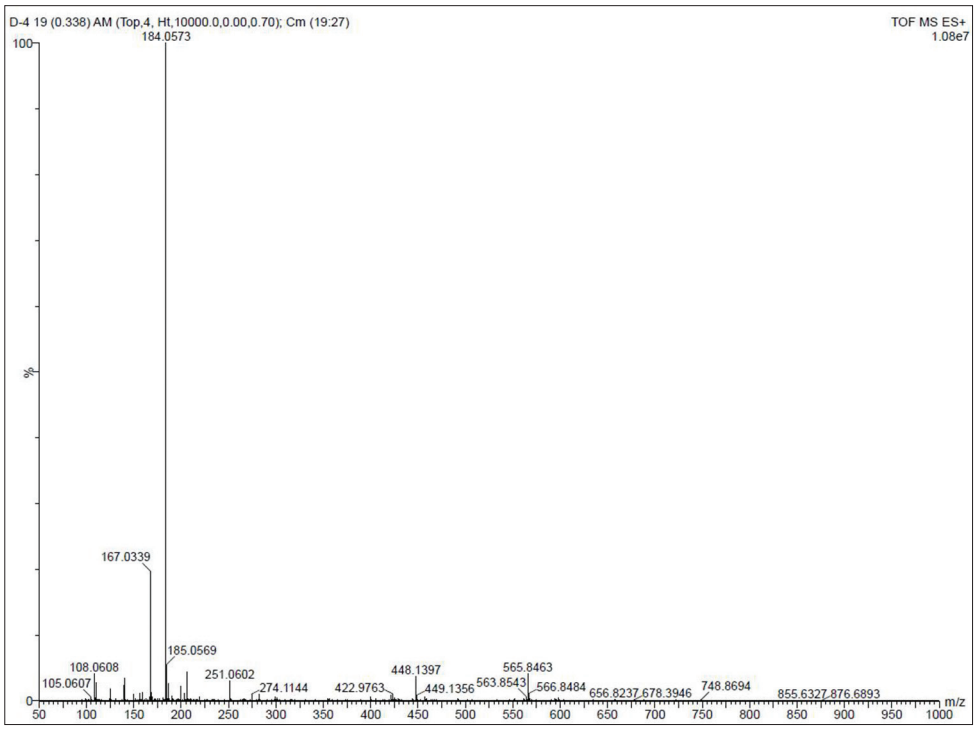

Supplementary Fig. 14: MASS spectra of D4

Supplementary Fig. 15: Antibacterial activity for *E. coli*

Supplementary Fig. 16: Antibacterial activity for *S. aureus*

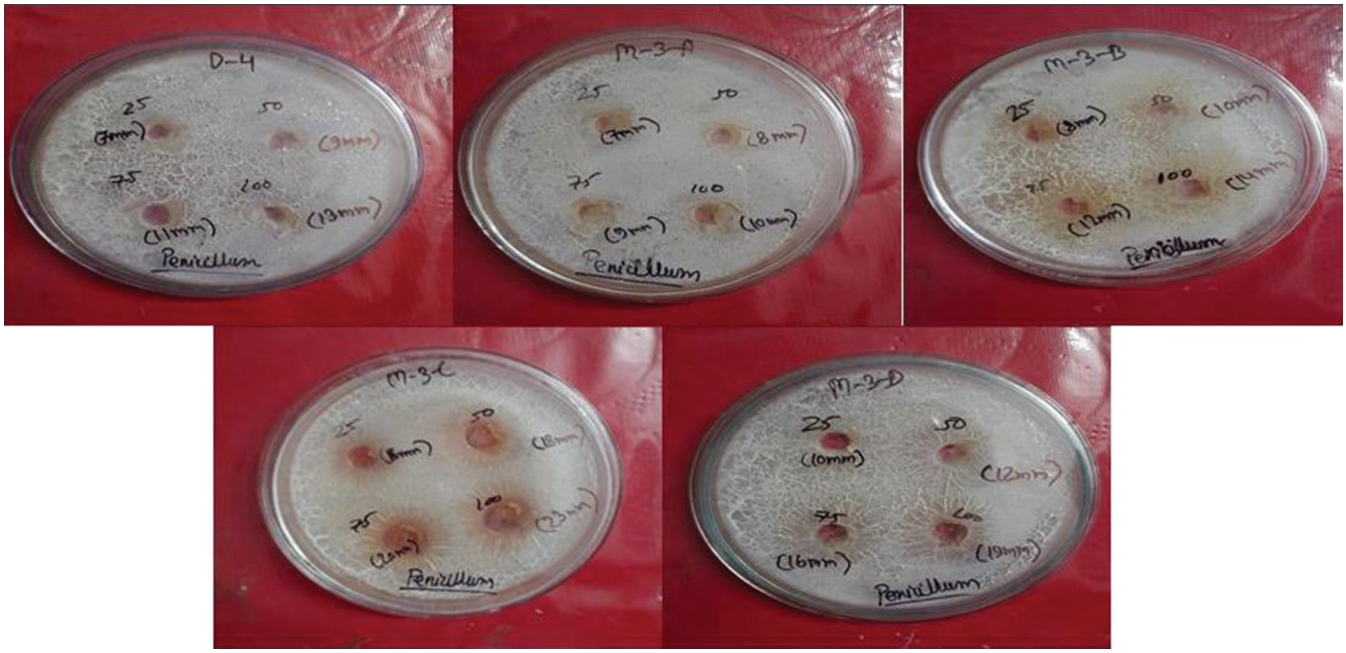

Supplementary Fig. 17: Antifungal activity for *P. chrysogenum* (std drug missing)

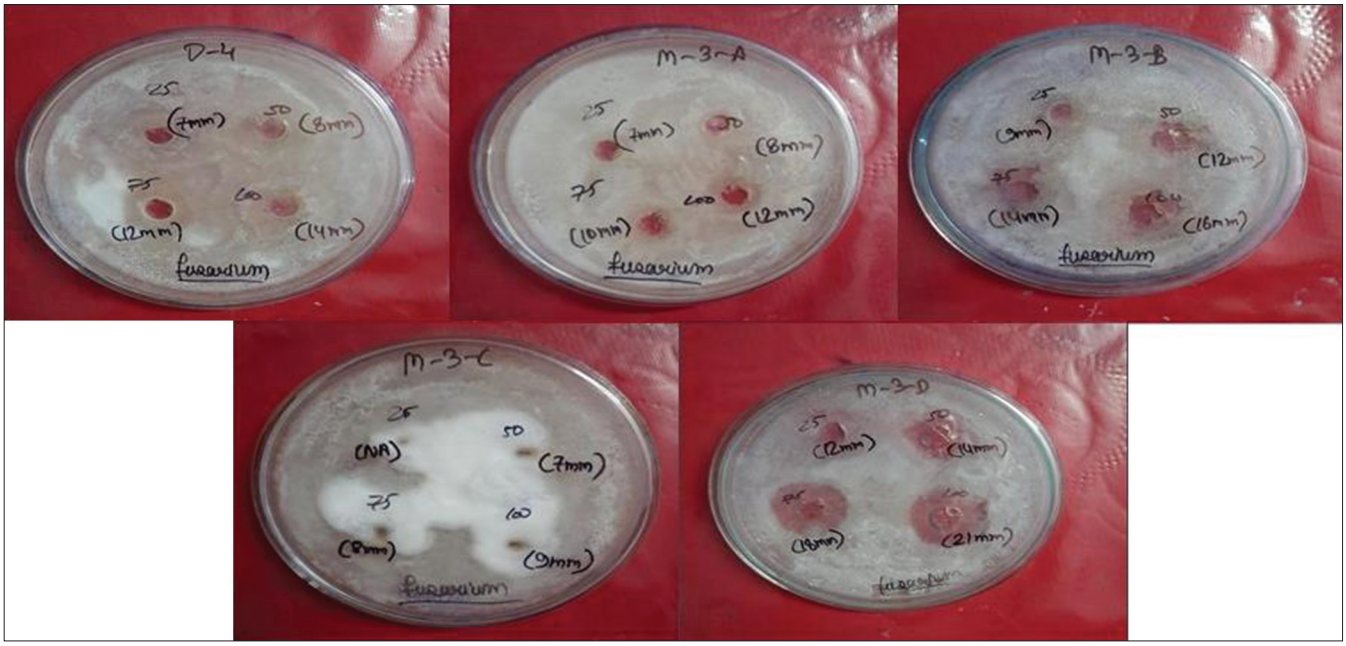

Supplementary Fig. 18: Antifungal activity for *F. oxysporum* (std drug missing)